Supporting Information

Mruk et al. 10.1073/pnas.1207606109

SI Text

SI Materials and Methods. ***Calmodulin (CaM) expression and purification.*** CaM constructs were transformed and expressed in *Escherichia coli* strain BL21(DE3) (Stratagene). Protein expression was induced with 0.4-mM IPTG overnight at 20 °C. The bacterial pellet was resuspended in lysis buffer containing (in mM): 2 EDTA, 0.2 PMSF, 1 β-mercaptoethanol (βME), and 50 Tris•HCl, pH 7.5. Cells were lysed by sonification, clarified by centrifugation, and the supernatant adjusted to a final concentration of 5 mM $CaCl_2$. Supernatant was applied to a phenyl-Sepharose CL-4B column (GE Healthcare) equilibrated with (in mM) 5 $CaCl_2$, 0.1 NaCl, 1 βME, 50 Tris•HCl, pH 7.5. The column was washed with four column volumes of wash buffer containing (in mM): 0.1 $CaCl_2$, 0.1 NaCl, 1 βME, 50 Tris•HCl, pH 7.5, and then with four column volumes of wash buffer containing 0.5 mM NaCl. Proteins were eluted in buffer containing (in mM): 1 EGTA, 1 βME, 50 Tris•HCl, pH 7.5. Purified CaM was dialyzed against distilled water and lyophilized.

Tetraethylammonium (TEA) injection studies. Families of Q2/Q3 current were first measured by holding at −80 mV and stepping to a series of test potentials for 4 s in 20-mV increments, followed by a tail pulse at −30 mV. After recording, oocytes were injected with TEA so the final concentration was 1–10 mM and allowed to recover for 2 h at 16 °C. Families of current were then remeasured and the amount of block was determined for each oocyte. The IC_{50} value for internal block by TEA was calculated by plotting the amount of block at 40 mV and fitting the data to a hyperbola.

Calcium-binding assay. 300 μg of each CaM construct was preloaded with 5 mM $CaCl_2$ and applied to a phenyl-Sepharose CL-4B column (GE Healthcare). Fractions from the wash and elution buffers were collected in 5-mL increments, and 10 μL of each fraction was diluted with SDS/PAGE loading buffer containing 100 mM DTT, separated on a 15% SDS-polyacrylamide gel, and resolved by Coomassie staining.

CaM–Gly_n–QuatenaryAmmonium (QA) studies. For oocyte comparison. Families of Q2/Q3 current were first measured by holding at −80 mV and stepping to a series of test potentials for 4 s in 20-mV increments, followed by a tail pulse at −30 mV. After recording, oocytes were injected with CaM–Gly_7–QA, so the in ovo concentration was 3 μM, and allowed to recover for 2 h at 16 °C. Families of current were then remeasured and the amount of block was determined for each oocyte.

For distance measurements. Inhibition was determined by batch comparison of oocytes injected with channel mRNA alone versus channel mRNA with CaM–Gly_n–QA at an in ovo concentration of 13–18 μM. The percent inhibition obtained from each batch was plotted as a function of extended tether length for each modified CaM. The distance curve was fit to the Boltzmann equation to generate a midpoint distance ($d_{1/2}$).

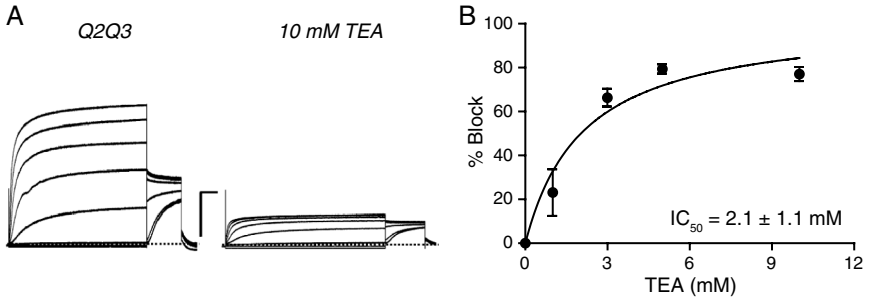

Fig. S1. Free TEA blocks Q2/Q3 channels internally at millimolar concentrations. (*A*) Families of currents recorded from *Xenopus* oocytes before and after injection of 10 mM TEA. Currents were elicited by 4-s test potentials from −100 to +40 mV in 20-mV increments from a holding potential of −80 mV followed by a tail pulse to −30 mV. Dashed line indicates zero current. Scale bars, 0.5 μA and 0.5 s. (*B*) Percent block at 40 mV was calculated for a range of TEA concentrations (1–10 mM). The IC_{50} value is reported as the mean ± the error of the fit to a hyperbola ($n = 4$–8).

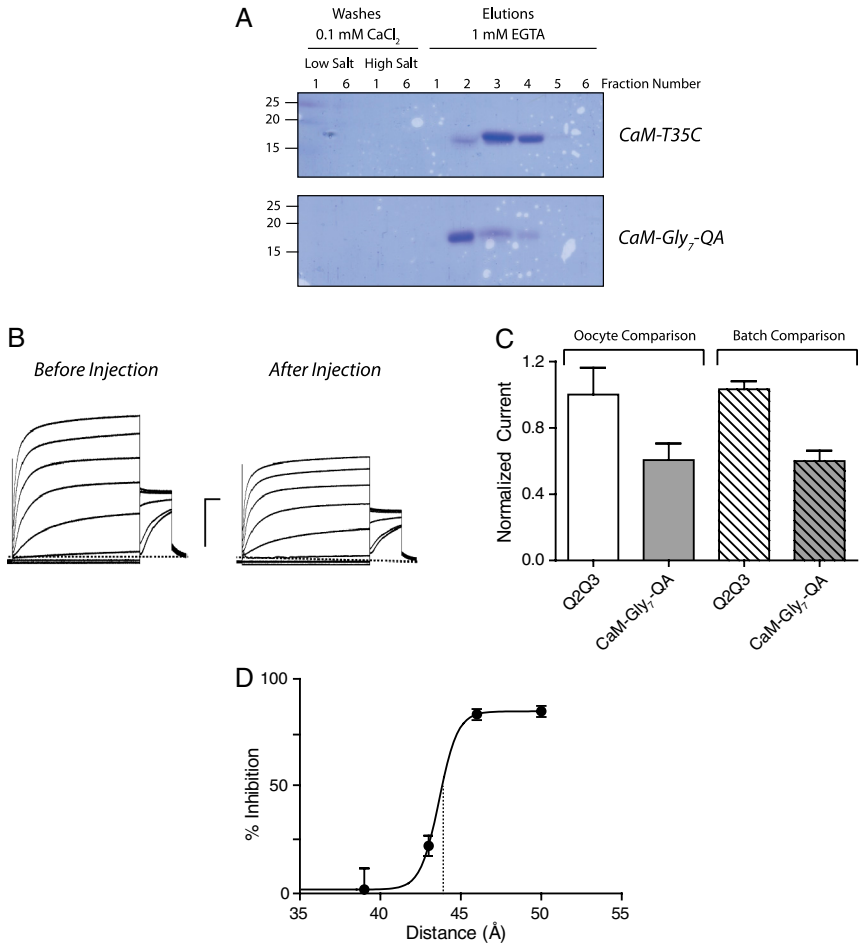

Fig. S2. QA-derivatized proteins retain calcium binding, exchange with endogenous CaM at the cell surface, and yield similar distance restraints when injected at in ovo concentrations that rival endogenous CaM. (*A*) Purified CaM binds to phenyl-Sepharose in the presence of calcium and dissociates upon chelation with EGTA. SDS/PAGE–resolved fractions from a phenyl-Sepharose column loaded with underivatized or derivatized CaM. (*B*) Families of Q2/Q3 currents recorded before and after injection of 3 μM CaM–Gly_7–QA. Currents were elicited by 4-s test potentials from −100 to +40 mV in 20-mV increments from a holding potential of −80 mV followed by a tail pulse to −30 mV. Dashed line indicates zero current. Scale bars, represent 0.5 μA and 0.5 s. (*C*) Inhibition of Q2/Q3 current by CaM–Gly_7–QA is not dependent on time of injection. Quantification of current levels from oocytes injected with CaM–Gly_7–QA. For oocyte comparison, values are normalized to current levels before injection. Batch comparison data is from Fig. 3 for comparison. Data are presented as the mean ± SEM from six individual oocytes. (*D*) Distance measurement of CaM residue T35 at higher concentrations (13–18 μM) of injected CaM–Gly_n–QA. Percent inhibition values plotted as a function of end-to-end linker length. Data are presented as the mean ± SEM from 1–2 batches of oocytes. The data were fitted to a Boltzmann equation to generate the midpoint of inhibition ($d_{1/2}$): T35C, 43 ± 1 Å.

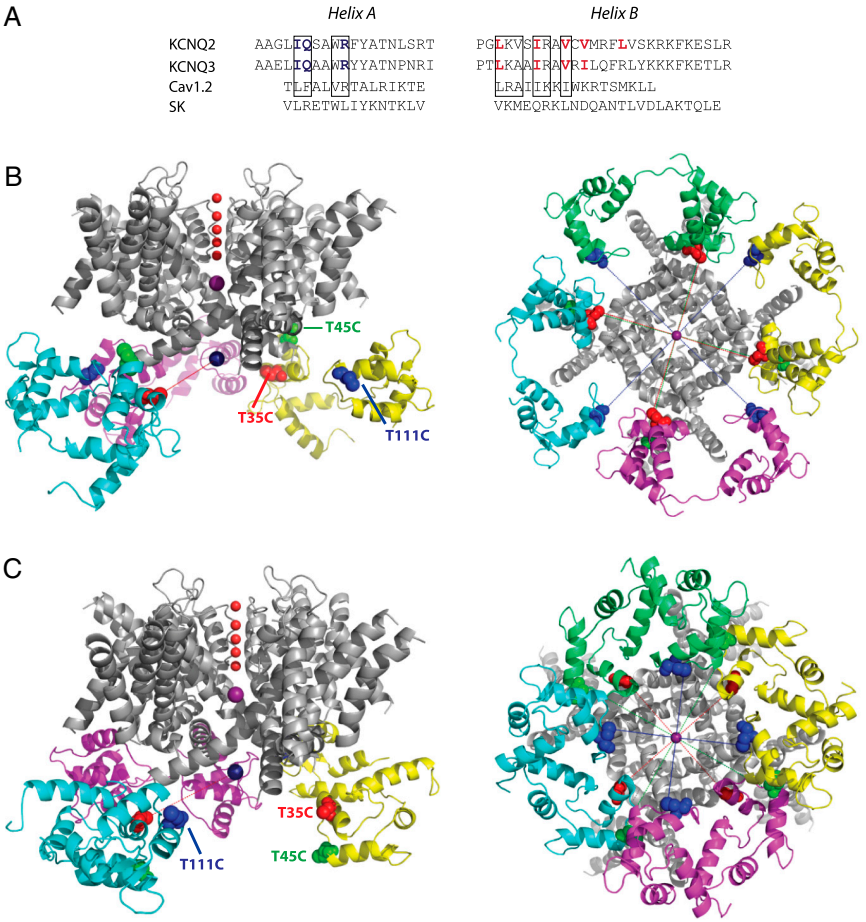

Fig. S3. Structural models of the Q2/Q3–CaM complex using the SK crystal structure [Protein Data Bank (PDB) 1G4Y]. Distance restraints were systematically loosened by 5 Å to prevent nonnative contacts. (*A*) CaM-binding motifs from Q2, Q3, Cav1.2, and SK channels. The IQ and 1-5-10 motifs in Q2/Q3 are highlighted. (*B*) Membrane and cytoplasmic views of the complex, showing the channel subunits colored grey and the four CaM molecules in different pastels. In the side view, only three subunits are shown for clarity. Residues T35C (red), T45C (green), and T111C (blue) are shown in space fill. Red spheres, potassium ions; purple sphere, TEA-binding site; blue sphere, dummy ion to simulate trajectory of the tethered blocker. (*C*) Membrane and cytoplasmic view of the complex with CaM subunits inverted. Colors are the same as in *B*.

Table S1. Mass spectrometry data*

Construct	Length (Å)	MW (Da) calculated	MW (Da) observed
CaM–Gly_3–QA	32	17,343	17,343
CaM–Gly_5–QA	39	17,457	17,456
CaM–Gly_6–QA	43	17,516	17,518
CaM–Gly_7–QA	46	17,571	17,572
CaM–Gly_8–QA	50	17,630	17,632
CaM–Gly_9–QA	54	17,687	17,687
CaM–Gly_{10}–QA	58	17,743	17,746
CaM–Gly_{11}–QA	62	17,803	17,803
CaM–Gly_{12}–QA	66	17,857	17,860
BM–Gly_7–QA	46	11,382	11,382

*Electrospray MS results for labeled CaM constructs. Observed masses were the same (within 1 Da) for all three threonine to cysteine mutants (T35C, T45C, T111C). MM, molecular mass.

Table S2. Distances between CaM residues and the Q2/Q3 TEA-binding site*

	$d_{1/2}$ (Å)		
Voltage (mV)	T35C	T45C	T111C
−20	40	48	49
0	41	48	49
20	41	48	49
40	40	49	50
Average	**41**	**48**	**49**

*Data from individual inhibition curves obtained from two to four batches of oocytes. Curves were fitted to a Boltzmann function to yield $d_{1/2}$ as described for Fig. 4.

Other Supporting Information Files

KCNQ_Cav_Model. Quaternary model was built using $rK_v2.1$ crystal structure (PDB: 2A79) and CaM bound to pre-IQ domain of $Ca_v1.2$ (PDB: 3G43) and used to generate Fig. 4*A*.

Dataset S1 (PDB)

KCNQ_InvertedCav_Model. Quaternary model was built using $rK_v2.1$ crystal structure (PDB: 2A79) and CaM bound to pre-IQ domain of $Ca_v1.2$ (PDB: 3G43). In this model, each CaM is inverted. This PDB was used to generate Fig. 4*B*.

Dataset S2 (PDB)

KCNQ_SK_Model. Quaternary model was built using $rK_v2.1$ crystal structure (PDB: 2A79) and CaM bound to the CaM-binding domain of SK2 (PDB: 1G4Y) and used to generate Fig. S3*B*.

Dataset S3 (PDB)

KCNQ_InvertedSK_Model. Quaternary model was built using $rK_v2.1$ crystal structure (PDB: 2A79) and CaM bound to the CaM-binding domain of SK2 (PDB: 1G4Y). In this model, each CaM is inverted. This PDB was used to generate Fig. S3*C*.

Dataset S4 (PDB)